To measure the concentration of dye in the anterior chamber, the eye of the euthanized rat was first washed with excess saline before a 30 gage needle was inserted into the anterior chamber through the boundary between the cornea and conjunctiva. The collected anterior chamber humor was mixed with the NaOH–DMSO solution in the volume ratio of 5 μl of aqueous humor per 2 ml of the NaOH–DMSO solution. The solution was then passed through a syringe filter (0.22 μm pore size) and the fluorescence spectra were measured. Ocular globes and eye fragments that were not treated with eye drop administration were used as controls.

2.7. Calculation of ocular penetration rates of dyes

The ocular penetration rates and the dye transition rates (Tables 1–4) of the dyes after administration of eye drops were calculated with the following formula (Eq. (1)):

$$\text{Ocular penetration rate of dye (\%, w/w)} = (\text{the weight concentration of actual dye penetration} \div \text{the weight concentration of the theoretical dye penetration}) \times 100 \quad (1)$$

Here, the "the weight concentration of actual dye penetration" means the real weight concentration of dyes detected in the specimen of the ocular globe and the eye segments, which were calculated using the calibration curve (see, Section 2 Material and methods; Section 2.6); the "the weight concentration of the theoretical dye penetration" means the virtual weight concentration of dyes with an assumption of complete dye transition to the ocular globe after administration of eye drops; i.e., this weight concentration was calculated based on the dye concentration of eye drops (10 μl) that was administered to the eye, and that were calculated using the calibration curve (see, Section 2 Material and methods; Section 2.4).

The calibration curves used for measurement of the ocular penetration rate of the dyes and the concentration of dyes in the anterior humor are shown in Supplementary Information Fig. S3a and S3b, respectively.

For statistical treatment of the data obtained on the ocular penetration rate and the dye distribution in eye segments, t-tests were carried out to investigate the probability (p) of significance. All p values obtained by the t-tests were based on analyzing multiple groups consisting of 5–6 samples for each p value. These p values are shown in Tables 1 to 4.

2.8. Fluorescence and confocal laser fluorescence microscopy observation

For the fluorescence microscopy observation of the ocular surfaces (Fig. 3), eye drops (10 μl) were administered to the eyes of anesthetized rats, and then after a given time, the eyes were observed by fluorescence microscopy (Zeiss, SteREO Lumar. V12). For confocal laser fluorescence microscopy (Figs. 5–7), ocular globes excised from euthanized rats were placed on glass-bottom dishes (35 mm, Corning) with the corneal side on the glass before the cross-section of the cornea was observed directly by confocal laser fluorescence microscopy (Olympus, FV-300). The laser source used in the experiment was an Ar laser with a 488 nm wavelength. A band pass filter (Olympus, BA510IF) was used to remove any excitation leakage. The series of fluorescence images obtained by both fluorescence and confocal laser fluorescence microscopy were confirmed as not being auto fluorescence of the cells and tissues; this was confirmed by comparing the ocular globes without staining dye as a control.

Table 1
Ocular penetration rates (%, w/w) of dyes after the administration of FDA nanoparticle and FDA microparticle eye drops.

Types of eye drops	Time after administration of eye drops			
	5 min	30 min	60 min	120 min
	Mean value of ocular penetration rate (%, w/w)			
FDA nanoparticles	9.00*,†	4.80*,†	3.45*,†	1.32*,†
FDA microparticles	0.18***	0.14**	0.12**	0.09**

Concentration of administered eye drops was 0.17 mg/ml.
Number of samples used for calculating each mean value: n = 6; except FDA microparticles at 5 min: n = 5.
* T test: $p<0.0001$ vs. control.
** T test: $p<0.005$ vs. control.
*** T test: $p<0.05$ vs. control.
† $p<0.0001$ vs. FDA microparticles.

Table 2
Ocular penetration rates of dyes after the administration of fluorescein nanoparticles and sodium fluorescein eye drops.

Type of eye drops	Time after administration of eye drops			
	5 min	30 min	60 min	120 min
	Mean value of ocular penetration rate (%, w/w)			
Fluorescein nanoparticles	0.18**	0.09**	0.10**	0.05**
Sodium fluorescein	0.16*	0.07**	0.07**	0.04**

Concentrations of administered fluorescein nanoparticle eye drops and sodium fluorescein eye drops were 0.29 mg/ml and 0.36 mg/ml, respectively.
Number of samples used for calculating each mean value: n = 6.
* T test: $p<0.0001$ vs. control.
** T test: $p<0.005$ vs. control.

3. Results and discussion

3.1. Evaluation of the size and morphology of FDA nanoparticles and FDA microparticles

FDA nanoparticles were prepared by the reprecipitation method [31–33]. Scanning electron microscopy (SEM) showed that the morphology of FDA nanoparticles prepared by the reprecipitation method was spheroidal (Fig. 2a). Dynamic light scattering (DLS) measurements showed that nanoparticle sizes were monodispersely distributed with an average size of 215 nm and that the ζ-potential of the system was −10 mV (Fig. S4, Supplementary Information). These nanoparticles were stably dispersed in aqueous medium because of a negatively charged ζ-potential as well as stabilizer PVP. These nanoparticles were stably dispersed in aqueous medium as shown in the photograph in Fig. 1 a-i. On the other hand, particles not formed by the reprecipitation method had a poor morphology. SEM showed that these particles were angular rather than spheroidal and that their size distribution spread across several micrometers. These results are shown in Fig. 2b, and the particles are referred to as microparticles in the remainder of this work. For the administration of eye drops to the eyes of rats, nanoparticle and microparticle eye drops were used

Table 3
Localization of dye obtained from each eye segment after administration of FDA nanoparticle eye drops.

Eye segments	Time after administration of eye drops			
	5 min	30 min	60 min	120 min
	Mean value of dye transition rate (%, w/w)			
Anterior eye	7.07*	6.06*	3.16*	1.45*
Sclera	0.04**	0.02*	0.01*	0.01***
Retina	0.02***	-	-	-

Concentration of administered FDA nanoparticle eye drops was 0.28 mg/ml.
Number of samples used for calculating each mean value: n = 6.
* T test: $p<0.0001$ vs. control.
** T test: $p<0.005$ vs. control.
*** T test: $p<0.05$ vs. control.

Table 4
The localization of dye obtained from frozen eye segments after administration of FDA nanoparticle eye drops.

Eye segments	Time after administration of eye drops			
	5 min	30 min	60 min	120 min
	Mean value of dye transition rate (%, w/w)			
Anterior eye	4.70*	3.56*	2.99*	0.78*
Conjunctiva–Sclera	0.31***	0.12**	0.04***	0.02***
Vitreous body	–	–	–	–
Retina	0.01***	–	–	–

Concentration of administered FDA nanoparticle eye drops was 0.42 mg/ml.
Number of samples used for calculating each mean value: n = 6.
* *T* test: $p<0.0001$ vs. control.
** *T* test: $p<0.005$ vs. control.
*** *T* test: $p<0.05$ vs. control.

before hydrolyzation and, therefore, the non-hydrolyzed FDA shows no fluorescence before their administration.

3.2. Fluorescein nanoparticles and sodium fluorescein eye drops

To examine the influence of polarity on the ocular penetration of eye drops, both fluorescein nanoparticles and sodium fluorescein eye drops were prepared for comparison with the FDA eye drops. The polarity of the chemical compound was described using octanol/water partition coefficient, log *P*. The log *P* of fluorescein is 0.61 and that of sodium fluorescein is −0.67 [39,40]. Since the log*P* of FDA is 3.51 [40], fluorescein and sodium fluorescein can be regarded as more hydrophilic than FDA because they have lower partition coefficients. Actually, fluorescein and sodium fluorescein are slightly and highly soluble in water, respectively. The average size of the fluorescein nanoparticles was 14 nm (Fig. S5, Supplementary Information) and sodium fluorescein in solution was molecular in size.

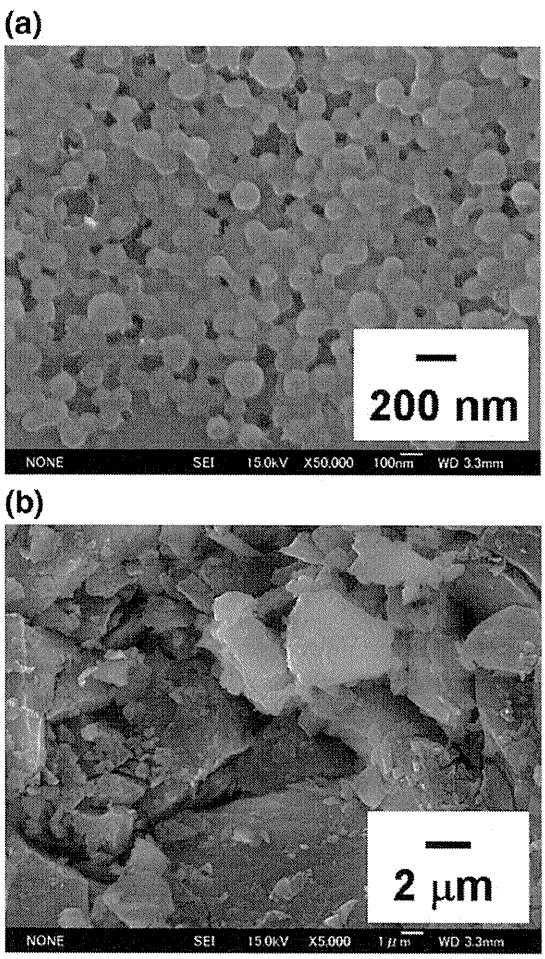

Fig. 2. SEM images of FDA nanoparticles (a) and FDA microparticles (b).

3.3. Fluorescence microscopy observation of ocular surfaces

Ocular surface images after administration of the eye drops are shown in Fig. 3. Fluorescence was not detected in the period from 10 s to 2 min after the administration of FDA nanoparticle eye drops, but was observed after 5 min (Fig. 3a). This fluorescence remained observable after the eye was washed using excess saline (Fig. 3a). In contrast, significant fluorescence was not detected in the ocular globe even at 5 min after the administration of FDA microparticle eye drops (Fig. 3b). Although the concentrations of FDA nanoparticle and FDA microparticle eye drops were the same, these results indicate that the particle size of FDA had a significant effect upon the rate of ocular penetration of the dye.

For both cases, fluorescence was detected at 10 s to 5 min after eye drop administration, but fluorescence was not detected after washing out the eyes with excess saline (Fig. 3c and d). This result indicated the dye in eye drops of fluorescein nanoparticles and sodium fluorescein did not permeate the epithelium. This means that the hydrophilic moieties present in their structure was not preferable for their penetration into the lipophilic corneal epithelium.

Additionally, the observation result using fluorescein eye drops eliminated the chance that the hydrolyzed FDA nanoparticles, which generate fluorescein outside of the ocular globe, entered into the corneal epithelium. Namely, it is clear that the dyes of the FDA nanoparticles were initially taken up by corneal epithelium cells and then the dyes were hydrolyzed inside the cells.

3.4. Quantitative analysis of the ocular penetration rate after administrating eye drops

The ocular penetration rates of FDA nanoparticle and microparticle eye drops were evaluated by quantitative analysis by means of measuring the fluorescence intensity of prepared specimens at a given time after administration of the eye drops (see, Section 2 Material and methods; Section 2.6). The highest fluorescence intensity was observed at 5 min after administering both eye drops (Fig. 4a). Additionally, the fluorescence intensity of FDA microparticle eye drops was less than that of FDA nanoparticles in all measurement times after their administration (Fig. 4b). The fluorescence intensity of both eye drops decreased as time elapsed (Fig. 4b). The temporal ocular penetration rates of these dyes are summarized in Table 1. The ocular penetration rate of dyes in FDA nanoparticles eye drops (9.00% w/w) was several times higher (ca. 50-fold) than that of the FDA microparticles (0.18% w/w) at 5 min after administration (Table 1). This shows that the downsizing of particles from a micrometer to a nanometer scale resulted in achieving high ocular penetration of dyes. This may mean that the dissolution rate of dyes from these particles on the ocular surface was greater for nanoparticles compared with that of microparticles because of a size effect, and then the dyes originating from the nanoparticles permeated into the corneal epithelium. Otherwise, nanoparticles being taken up into the corneal epithelium cells are considered to have occurred in the case of nanoparticle eye drops. The dyes and particles that did not migrate to the ocular globe were washed away from the eye surface by the actions of lacrimation and tear turnover. Similarly, the reason for the reduction of the dye amount observed in the ocular globe over time may be due to the action of aqueous flow in removing the dye and to

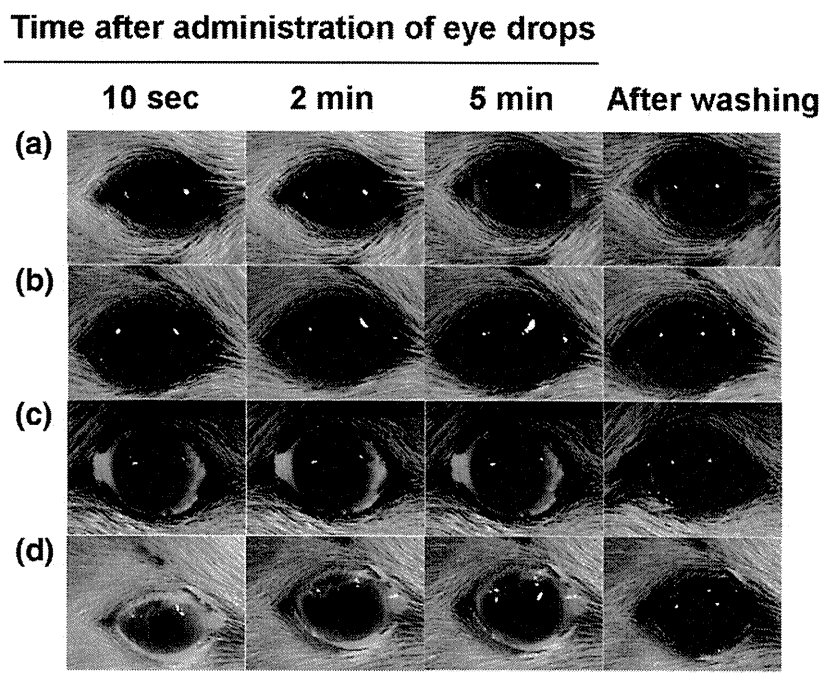

Fig. 3. Fluorescence microscopy images of the ocular surfaces after eye drop administration. The applied eye drops were FDA nanoparticles (a), FDA microparticles (b), Fluorescein nanoparticles (c), and sodium fluorescein (d). Concentration of administered eye drops was 0.47 mM (number of molecules) in each case.

the diffusion of dye into the blood circulation. These mechanisms have been recognized in previous research [11].

The ocular penetration rates of fluorescein nanoparticles and sodium fluorescein were weak during the 2 h following eye drop administration (Table 2 and corresponding graphs in Fig. S6, Supplementary Information). These results are consistent with the existing literature that describes the cornea permeability of chemical compounds according to the log *P*. Since the log *P* of fluorescein and sodium fluorescein is 0.61 and −0.67, respectively, it has been found that compounds with log *P* values of around 2–3 penetrate the cornea more readily [41,42]. Even though, the sizes of fluorescein nanoparticles (ca. 14 nm in size) and sodium fluorescein (molecular in size) were smaller than that of FDA nanoparticles (ca. 215 nm in size), the ocular penetration rate was less than that of FDA nanoparticles. This result means that not only the size but also the polarity of the compound is an important factor for determining the ocular penetration of dyes.

3.5. Confocal laser fluorescence microscopy of the cornea

Since the cornea is a transparent tissue, it is possible to observe a cross section of the tissue using confocal laser fluorescence microscopy. When administrating FDA nanoparticle eye drops, deep cornea penetration of dyes was observed (Fig. 5a; the detailed discussion is in a Section 3.6). For the other types of eye drops studied (i.e., FDA microparticles, fluorescein nanoparticles, and sodium fluorescein), only confocal fluorescence images of surfaces of the superficial corneal epithelium were taken (Fig. 5b–d) and these results showed that the permeation of these dyes through the epithelium was low. Thus, less ocular penetration took place.

3.6. Fluorescence imaging of corneal cross-sections after administrating FDA nanoparticle eye drops

Among the four types of eye drops used in this study (FDA nanoparticles, FDA microparticles, fluorescein nanoparticles, and sodium fluorescein), FDA nanoparticle eye drops were found to have the highest ocular penetration rate. We therefore focused on investigating FDA nanoparticle eye drops. Sixty minutes after the administration of FDA nanoparticle eye drops, a fluorescence image of the corneal cross section was taken that depicted the epithelium, stroma, and endothelium (Fig. 6a). The corresponding fluorescence intensity distribution curve in the cornea and plane view images of each layer are shown in Fig. 6b and Fig. 6c-i, respectively. The depths of plane view images of Fig. 6c-i correspond with the lower-case labels c-i in yellow in Fig. 6a. In the corneal epithelium, the dyes were observed in the cell cytoplasm in the superficial layer (Fig. 6c) and intercellular spaces in the suprabasal and basal layers (Fig. 6d and e). FDA might have been taken up by the corneal epithelium cells in the form of FDA molecules originating from the dissolved nanoparticles on the corneal surface and/or in the form of FDA nanoparticles. It is speculated that the molecular dyes and/or the nanoparticles were hydrolyzed in the cytoplasm of cells in the superficial layer, then the hydrolyzed dyes and/or the nanoparticles having hydrolyzed a surface of fluorescein were exocytosed. These dyes and fluorescent nanoparticles might have passed through the intercellular spaces of the suprabasal and basal layers because their hydrophilic moiety, caused by fluorescein, made it difficult to reenter the cells that were covered by the lipophilic membrane. Fig. 6f and g shows fluorescent dots that may be the aggregation of fluorescent nanoparticles that had hydrolyzed and thus had a fluorescent surface of fluorescein. The sizes of aggregation substances were estimated to be up to several micrometers. For easier viewing, these fluorescent aggregate substances between the basal epithelium layer and stromal layers are enlarged in Fig. 6g and highlighted inside yellow circles. This result indicates the possibility of direct nanoparticle permeation into the corneal epithelium. Since these fluorescent aggregates were trapped in the boundary between the epithelium and stroma (see, lower-case labels f and g in Fig. 6a, and f and g), the hydrophilic fluorescein dyes produced by the hydrolyzed FDA of the nanoparticles might have dominantly permeated through the hydrophilic stroma (Fig. 6h). Then these dyes reached the endothelium (Fig. 6i).

To investigate the details of dye transition from the epithelium to the stroma, a three-dimensional image was taken using the alpha blend method (Fig. 7a). Again, this image shows the passage of

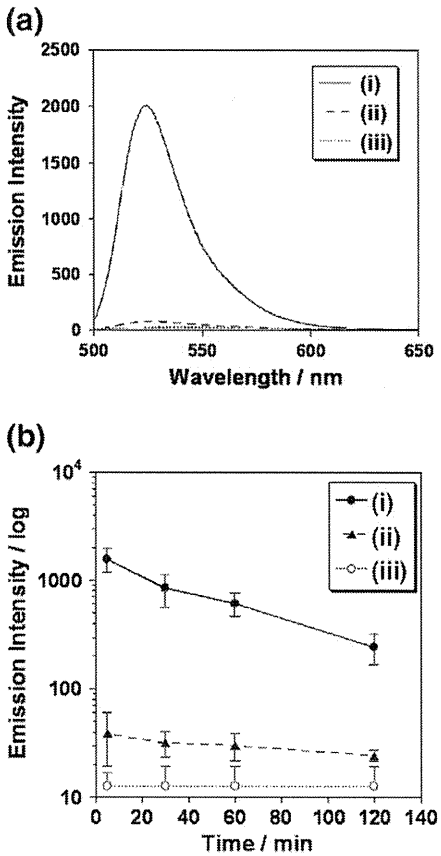

Fig. 4. Emission spectra of dye solution from excised ocular globes at 5 min after eye drop administration (a): FDA nanoparticles (i) and FDA microparticles (ii) eye drops and control (without staining dyes) (iii). Dye transition to the ocular globe at 5, 30, 60, and 120 min after eye drop administration (b): detecting at the λ_{max} (=525 nm) of the florescence spectra for the case of administration of FDA nanoparticles (i) and FDA microparticles (ii) eye drops and control (without staining dyes) (iii); each point value represents the mean ± s.d., and n = 6, except (ii) at 5 min (n = 5).

fluorescent dye through the intercellular spaces between the epithelium. Additionally, fluorescent distributions and fluorescent images of the epithelium (Fig. 7b) revealed that most dyes were absorbed by the superficial layer (Fig. 7b-i) and passed through the intercellular spaces of the suprabasal and basal layers (Fig. 7b-ii and b-iii). The red arrow in Fig. 7b-ii shows a fluorescent cell. This example cell shows that some dyes were taken up by cells in the suprabasal layer. It seems that some dyes and/or nanoparticles might have passed through the tight junctions, and then entered the cell in the suprabasal layer, followed by being hydrolyzed inside the cytoplasm. Although tight junctions work as a good barrier for substances external to the epithelium [43], dye clusters and/or small sized nanoparticles can pass through the pores existing between these tight junctions [43] rather than becoming entrapped in the cells of the superficial layer of the epithelium. However, the exact mechanism for this penetration is still being investigated. Additionally, the cell that took up the dyes and/or nanoparticles in the suprabasal layer were easily observable in the transparent three-dimensional image obtained using the maximum intensity projection method (Fig. 7c, the fluorescent cell is shown by the red arrow). The fluorescent cell in Fig. 7c corresponds with that of Fig. 7b-ii.

Fluorescein dyes produced by hydrolysis of FDA permeated through the hydrophilic stroma, which was confirmed by both the alpha blend method (Fig. 7a) and the maximum intensity projection method (Fig. 7c). These results mean that the formulation of nanoparticles of a hydrolyzable compound can overcome the corneal barrier functions, which consist of the tight junctions of the corneal epithelium as well as the different physicochemical properties of the lipophilic epithelium and the hydrophilic stroma.

At present, there are numerous reports discussing the ocular penetration of dyes, nanoparticles, and drugs [9,14,30,44–51]. However, to the best of our knowledge, this is the first time confocal laser fluorescence microscopy was used to clearly visualize the unique penetration pathway of the compounds consisting of nanoparticles with hydrolyzable dyes through the cornea.

3.7. Dye localization in the ocular globe

After administering FDA nanoparticle eye drops and waiting for a given time, the eyes were washed with saline before and after excising the ocular globe. The excised ocular globe was carefully dissected under a microscope to obtain the anterior segment, conjunctiva, sclera, retina, and vitreous body (see, Section 2 Material and methods; Section 2.6). The ocular penetration rate of the dyes in these fragments was determined by quantitative analysis using fluorescence spectra measurements and calibration curves.

Table 3 shows that almost all the dye was found in the anterior segment (e.g., the ocular penetration rate was 7.07% w/w at 5 min), although some dyes reached the sclera and the retina of the posterior eye segment (corresponding graphs are shown in Fig. S7a–S7c, Supplementary Information). Dye was detected in the retina 5 min after administration of FDA nanoparticle eye drops; however, no significant signal was detected after 30 min.

An additional experiment using a frozen ocular globe was performed to reduce the chance of false results due to contamination (see, Section 2 Material and methods; Section 2.6). A similar trend in the ocular penetration of dyes was observed using this technique. Again, most of the dye was detected in the anterior eye segment (e.g., ocular penetration rate was 4.70% w/w at 5 min), while the remainder was detected in the conjunctiva, sclera and retina (Table 4 and the corresponding graphs in Fig. S8, Supplementary Information). Fig. S8d shows that significant fluorescence in the vitreous body of the posterior eye segment was not detected.

The ocular penetration rate of dyes in the anterior chamber after the administration of eye drops was investigated by measuring the dye concentration in the aqueous humor using the calibration curve (Supplementary Information S3b). As a result, 30 min after the administration of FDA nanoparticle eye drops, the aqueous humor was found to have the highest concentration of the dye (0.56 ± 0.24 μg/ml). The changes in fluorescence intensity and the concentration of dye in the aqueous humor over time are summarized in Table 5 and corresponding graphs are shown in Supplementary Information Fig. S7d.

3.8. Transport of dye to the retina

Drug delivery to the retina using eye drops is an ideal delivery method since administration of drugs to the retina are often limited to oral administration, intravenous injection, and local administration (intravitreal injections/implants and periocular injections). These methods have associated risks of systemic toxicity and infections [52,53]. The anterior chamber of the eye is considered to be the main site at which the pharmacodynamic effects of eye drops take effect in intraocular tissue [12]. However, in this study, the dye might have migrated to the retina through the conjunctiva and sclera, and not through the anterior chamber since the greatest fluorescence intensity in our measurements of the retina was observed at 5 min after eye drop administration (0.02%, w/w; Table 3) and the maximum intensity measured from the anterior chamber was observed after 30 min (0.56 ± 0.24 μg/ml; Table 5 and Supplementary Information Fig. S7d). If the dye passed through the anterior chamber, the maximum fluorescence intensity in the retina should appear 30 min after the administration of

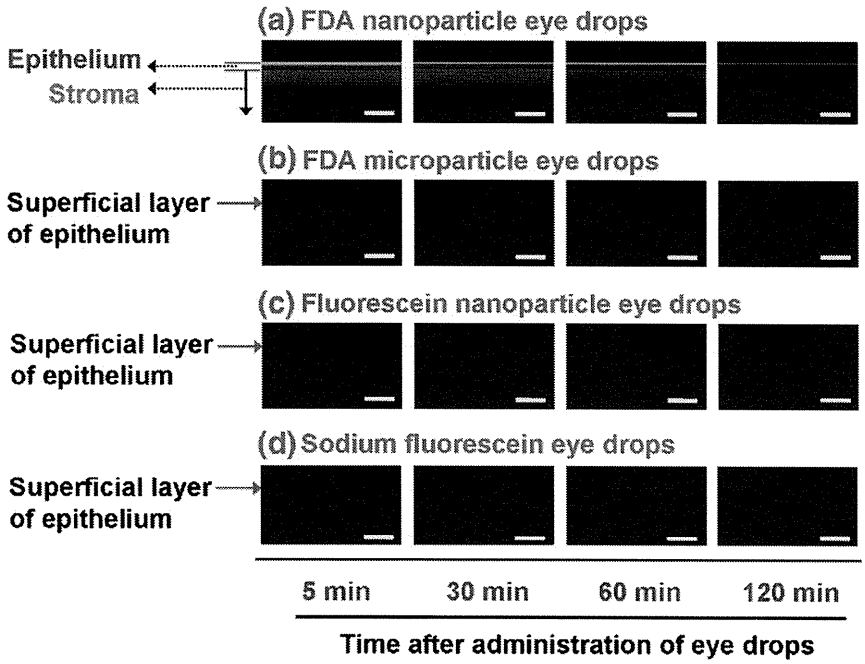

Fig. 5. Confocal laser fluorescence microscopy observation of corneal cross-sections at 5, 30, 60, and 120 min after administration of different types of eye drops. The administered eye drops were FDA nanoparticles (a), FDA microparticles (b), fluorescein nanoparticles (c), and sodium fluorescein (d). The concentration of each eye drops was 0.7 mM (number of molecules). The scale bar (yellow line) indicates 50 μm.

the eye drops. Furthermore, the fact that no significant fluorescent intensity was observed in the vitreous body eliminates the dye passing through the anterior chamber to the vitreous body, resulting in the dye reaching retina (Table 4 and Supplementary Information Fig. S8d). Since the conjunctiva and sclera are more permeable than the cornea, the main route of drug delivery to the retina has recently been considered to occur through the conjunctiva–sclera route [44,54–57]. These findings correspond to the results obtained for the FDA nanoparticle eye drops in this study. Furthermore, it has been reported that the drug transition rate to the retina is usually 0.001%–0.01% of the amount, even using

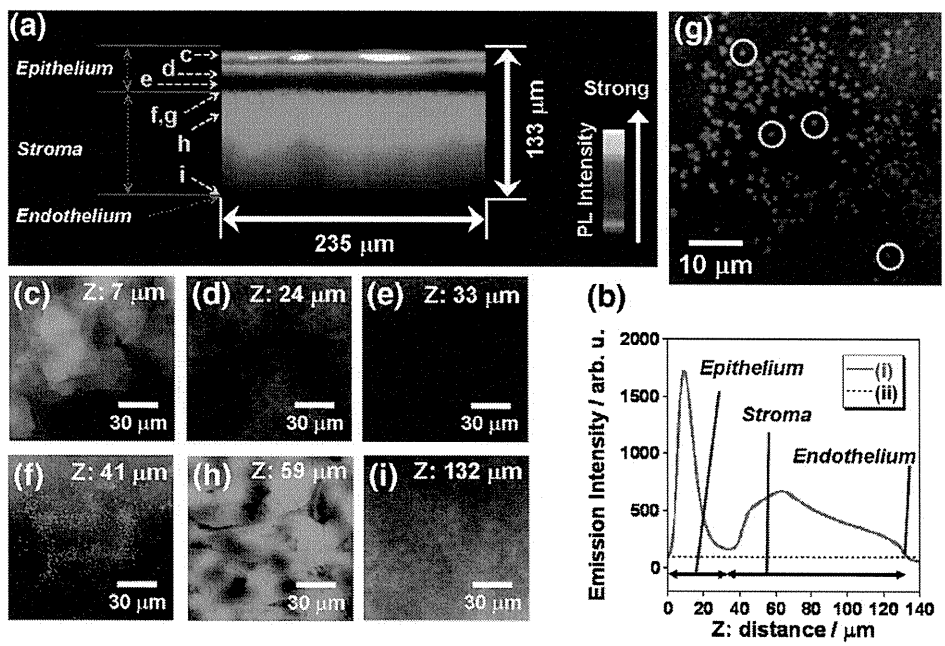

Fig. 6. Confocal laser fluorescence microscopy observation of a cornea. Cross-section image of the cornea at 60 min after administration of FDA nanoparticle eye drops (a) and corresponding fluorescence intensity curve, (b): fluorescence intensity curve vs. depth in cornea (i) and base line (ii). Corresponding superficial layer (c), suprabasal layer (d), and basal layer (e) in the epithelium; the phase between epithelium basal layer and stromal layer (f): enlarged view (g) (examples of aggregates of fluorescent nanoparticles are shown inside yellow circles); stroma (h), and endothelium (i). The concentration of FDA nanoparticles in the administered eye drops was 2.2 mg/ml.

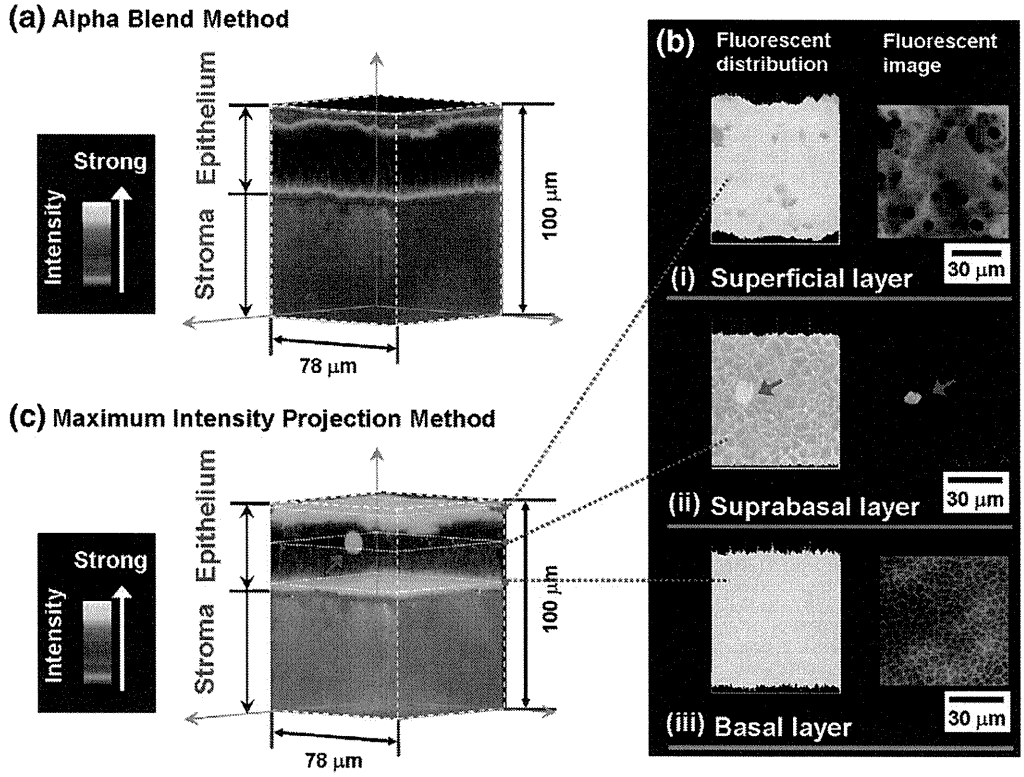

Fig. 7. Fluorescence images of the corneal epithelium at 30 min after administering FDA nanoparticles: three dimensional fluorescence cross sectional image of the cornea obtained by the rendering mode of the alpha blend method (a) and maximum intensity projection method (c); the corresponding fluorescent distributions and fluorescent images (b): superficial layer (i), suprabasal layer (ii), and basal layer (iii).

subconjunctival injection [38]. Therefore, eye drops using nanoparticles of hydrolyzable compounds targeting the retina can be assessed as a promising method for retinal drug delivery (transition rate was 0.01%–0.02% w/w as shown in Tables 3 and 4).

4. Conclusions

A method for enhancing the ocular penetration rate of eye drops through administration of nanoparticles of hydrolyzable dye; i.e., FDA, was described in this study. The FDA nanoparticles were shown to have high penetration rates. The formulation of the FDA nanoparticles overcame the problems of the corneal barrier function. Namely, the formulation of FDA nanoparticles overcame the problem of tight junctions as well as the physicochemical property of a lipophilic epithelium and a hydrophilic stroma. Important determinants of their penetrating ability through these corneal barrier functions were identified. The particle size and the change in the polarity of the dye from lipophilic to hydrophilic through corneal hydrolysis were identified as important. The unique penetration pathway of dyes and/or nanoparticles through the cornea was identified by confocal laser fluorescence microscopy. In the future, using nanoparticles of a hydrolyzable compound and employing an *in vivo* hydrolysis reaction not only can be used to improve drug penetration into ocular tissue, but may also be applied to other tissues that have specific barrier functions (e.g., the blood–brain barrier and epidermal barrier). Detailed investigations of ocular penetration and the effects of particle size and the polarity of nanoparticles; i.e., a nanoparticle-based unique penetration pathway and drug distribution, are currently underway in our laboratory with several kinds of ocular drugs being studied.

Table 5
Dye concentrations in the anterior humor at given times after the administration of FDA nanoparticle eye drops.

	Time after administration of eye drops			
	5 min	30 min	60 min	120 min
Concentration of dyes in the anterior humor (μg/ml)	0.21 ± 0.16	0.56 ± 0.24	0.50 ± 0.23	0.16 ± 0.01

Concentrations of administered FDA nanoparticle eye drops was 0.38 mg/ml.
Each value represents the mean ± s.d. (n = 6).

Acknowledgments

This study was partially supported by a Grants-in-Aid for Young Scientists B (No. 21700456) from the Japan Society for the Promotion of Science; Health and Labor Science Research Grants for Research on Intractable Diseases from the Ministry of Health, Labor and Welfare of Japan; and the Exploratory Research Program for Young Scientists from Tohoku University.

Appendix A. Supplementary data

Supplementary data to this article can be found online at doi: 10.1016/j.jconrel.2011.04.019.

References

[1] Y. Cu, W.M. Saltzman, Drug delivery: stealth particles give mucus the slip, Nat. Mater. 8 (2009) 11–13.
[2] S. Majumdar, A.K. Mitra, Chemical modification and formulation approaches to elevated drug transport across cell membranes, Expert Opin. Drug Deliv. 3 (2006) 511–527.
[3] A.E. Nel, L. Madler, D. Velegol, T. Xia, E.M. Hoek, P. Somasundaran, F. Klaessig, V. Castranova, M. Thompson, Understanding biophysicochemical interactions at the nano-bio interface, Nat. Mater. 8 (2009) 543–557.

[4] R.A. Petros, J.M. DeSimone, Strategies in the design of nanoparticles for therapeutic applications, Nat. Rev. Drug Discov. 9 (2010) 615–627.
[5] T. Xia, L. Rome, A. Nel, Nanobiology: particles slip cell security, Nat. Mater. 7 (2008) 519–520.
[6] Y. Ali, K. Lehmussaari, Industrial perspective in ocular drug delivery, Adv. Drug Deliv. Rev. 58 (2006) 1258–1268.
[7] C.L. Bourlais, L. Acar, H. Zia, P.A. Sado, T. Needham, R. Leverge, Ophthalmic drug delivery systems-recent advances, Prog. Retin. Eye Res. 17 (1998) 33–58.
[8] I.P. Kaur, M. Kanwar, Ocular preparations: the formulation approach, Drug Dev. Ind. Pharm. 28 (2002) 473–493.
[9] E. Mannermaa, K.S. Vellonen, A. Urtti, Drug transport in corneal epithelium and blood-retina barrier: emerging role of transporters in ocular pharmacokinetics, Adv. Drug Deliv. Rev. 58 (2006) 1136–1163.
[10] D.M. Maurice, Structures and fluids involved in the penetration of topically applied drugs, Int. Ophthalmol. Clin. 20 (1980) 7–20.
[11] S. Mishima, Clinical pharmacokinetics of the eye. Proctor lecture, Invest. Ophthalmol. Vis. Sci. 21 (1981) 504–541.
[12] Y. Shirasaki, Molecular design for enhancement of ocular penetration, J. Pharm. Sci. 97 (2008) 2462–2496.
[13] R. Gaudana, J. Jwala, S.H. Boddu, A.K. Mitra, Recent perspectives in ocular drug delivery, Pharm. Res. 26 (2009) 1197–1216.
[14] D. Ghate, H.F. Edelhauser, Ocular drug delivery, Expert Opin. Drug Deliv. 3 (2006) 275–287.
[15] P. Druzgala, D. Winwood, M. Drewniak-Deyrup, S. Smith, N. Bodor, J.J. Kaminski, New water-soluble pilocarpine derivatives with enhanced and sustained muscarinic activity, Pharm. Res. 9 (1992) 372–377.
[16] J. Araujo, E. Gonzalez, M.A. Egea, M.L. Garcia, E.B. Souto, Nanomedicines for ocular NSAIDs: safety on drug delivery, Nanomedicine 5 (2009) 394–401.
[17] H.Z. Bu, H.J. Gukasyan, L. Goulet, X.J. Lou, C. Xiang, T. Koudriakova, Ocular disposition, pharmacokinetics, efficacy and safety of nanoparticle-formulated ophthalmic drugs, Curr. Drug Metab. 8 (2007) 91–107.
[18] I.P. Kaur, A. Garg, A.K. Singla, D. Aggarwal, Vesicular systems in ocular drug delivery: an overview, Int. J. Pharm. 269 (2004) 1–14.
[19] J.E. Kipp, The role of solid nanoparticle technology in the parenteral delivery of poorly water-soluble drugs, Int. J. Pharm. 284 (2004) 109–122.
[20] N. Ueno, M.F. Refojo, M.B. Abelson, in: D.M. Albert, F.A. Jakobiec (Eds.), Principle and Practice of Ophthalmology, Basic Science, Chap. 74, W. B. Saunders, Philadelphia, 1994, pp. 916–929.
[21] R.D. Schoenwald, P. Stewart, Effect of particle size on ophthalmic bioavailability of dexamethasone suspensions in rabbits, J. Pharm. Sci. 69 (1980) 391–394.
[22] S. Wadhwa, R. Paliwal, S.R. Paliwal, S.P. Vyas, Nanocarriers in ocular drug delivery: an update review, Curr. Pharm. Des. 15 (2009) 2724–2750.
[23] S.K. Sahoo, F. Dilnawaz, S. Krishnakumar, Nanotechnology in ocular drug delivery, Drug Discov. Today 13 (2008) 144–151.
[24] L. Zhang, Y. Li, C. Zhang, Y. Wang, C. Song, Pharmacokinetics and tolerance study of intravitreal injection of dexamethasone-loaded nanoparticles in rabbits, Int. J. Nanomedicine 4 (2009) 175–183.
[25] A.A. Attama, S. Reichl, C.C. Muller-Goymann, Sustained release and permeation of timolol from surface-modified solid lipid nanoparticles through bioengineered human cornea, Curr. Eye Res. 34 (2009) 698–705.
[26] M.M. Bailey, C.J. Berkland, Nanoparticle formulations in pulmonary drug delivery, Med. Res. Rev. 29 (2009) 196–212.
[27] D.P. Cormode, T. Skajaa, Z.A. Fayad, W.J. Mulder, Nanotechnology in medical imaging: probe design and applications, Arterioscler. Thromb. Vasc. Biol. 29 (2009) 992–1000.
[28] S.S. D'Souza, P.P. DeLuca, Methods to assess in vitro drug release from injectable polymeric particulate systems, Pharm. Res. 23 (2006) 460–474.
[29] A. Nel, T. Xia, L. Madler, N. Li, Toxic potential of materials at the nanolevel, Science 311 (2006) 622–627.
[30] T.K. De, E.J. Bergey, S.J. Chung, D.J. Rodman, D.J. Bharali, P.N. Prasad, Polycarboxylic acid nanoparticles for ophthalmic drug delivery: an ex vivo evaluation with human cornea, J. Microencapsul. 21 (2004) 841–855.
[31] K. Baba, H.E. Pudavar, I. Roy, T.Y. Ohulchanskyy, Y. Chen, R.K. Pandey, P.N. Prasad, New method for delivering a hydrophobic drug for photodynamic therapy using pure nanocrystal form of the drug, Mol. Pharmaceutics 4 (2007) 289–297.
[32] K. Baba, H. Kasai, A. Masuhara, H. Oikawa, H. Nakanishi, Organic solvent-free fluorescence confocal imaging of living cells using pure nanocrystal forms of fluorescent dyes, Jpn. J. Appl. Phys. 48 (2009) 117002/1-117002/4.
[33] H. Kasai, H.S. Nalwa, H. Oikawa, S. Okada, H. Matsuda, N. Minami, A. Kakuta, K. Ono, A. Mukoh, H. Nakanishi, A novel preparation method of organic microcrystals, Jpn. J. Appl. Phys. 31 (1992) L1132–L1134.
[34] K.H. Jones, J.A. Senft, An improved method to determine cell viability by simultaneous staining with fluorescein diacetate-propidium iodide, J. Histochem. Cytochem. 33 (1985) 77–79.
[35] K.K. Sin, C.P. Chan, T.H. Pang, M. Seydack, R. Renneberg, A highly sensitive fluorescent immunoassay based on avidin-labeled nanocrystals, Anal. Bioanal. Chem. 384 (2006) 638–644.
[36] W. Cai, I.R. Gentle, G.Q. Lu, J.-J. Zhu, A. Yu, Mesoporous silica templated biolabels with releasable fluorophores for immunoassays, Anal. Chem. 80 (2008) 5401–5406.
[37] C.P. Chan, Y. Cheung, R. Renneberg, M. Seydack, New trends in immunoassays, Adv. Biochem. Eng. Biotechnol. 109 (2008) 123–154.
[38] D.M. Maurice, Drug delivery to the posterior segment from drops, Surv. Ophthalmol. 47 (Suppl 1) (2002) S41–S52.
[39] M. Araie, D. Maurice, The rate of diffusion of fluorophores through the corneal epithelium and stroma, Exp. Eye Res. 44 (1987) 73–87.
[40] A.K. Ho, L.E. Bromberg, A.J. O'Connor, J.M. Perera, G.W. Stevens, T.A. Hatton, Solute diffusion in associative copolymer solutions, Langmuir 17 (2001) 3538–3544.
[41] R.D. Schoenwald, R.L. Ward, Relationship between steroid permeability across excised rabbit cornea and octanol–water partition coefficients, J. Pharm. Sci. 67 (1978) 786–788.
[42] W. Wang, H. Sasaki, D.S. Chien, V.H.L. Lee, Lipophilicity influence on conjunctival drug penetration in the pigmented rabbit — a comparison with corneal penetration, Curr. Eye Res. 10 (1991) 571–579.
[43] S. Tsukita, M. Furuse, M. Itoh, Multifunctional strands in tight junctions, Nat. Rev. Mol. Cell Biol. 2 (2001) 285–293.
[44] K.M. Hamalainen, K. Kananen, S. Auriola, K. Kontturi, A. Urtti, Characterization of paracellular and aqueous penetration routes in cornea, conjunctiva, and sclera, Invest. Ophthalmol. Vis. Sci. 38 (1997) 627–634.
[45] A.M. De Campos, A. Sanchez, R. Gref, P. Calvo, M.J. Alonso, The effect of a PEG versus a chitosan coating on the interaction of drug colloidal carriers with the ocular mucosa, Eur. J. Pharm. Sci. 20 (2003) 73–81.
[46] P. Calvo, C. Thomas, M.J. Alonso, J.L. Vila-Jato, J.R. Robinson, Study of the mechanism of interaction of poly(ε-caprolactone) nanocapsules with the cornea by confocal laser scanning microscopy, Int. J. Pharm. 103 (1994) 283–291.
[47] C.A. Poole, N.H. Brookes, G.M. Clover, Confocal imaging of the human keratocyte network using the vital dye 5-chloromethylfluorescein diacetate, Clin. Exp. Ophthalmol. 31 (2003) 147–154.
[48] M. Sosnova-Netukova, P. Kuchynka, J.V. Forrester, The suprabasal layer of corneal epithelial cells represents the major barrier site to the passive movement of small molecules and trafficking leukocytes, Br. J. Ophthalmol. 91 (2007) 372–378.
[49] S. Speier, D. Nyqvist, M. Kohler, A. Caicedo, I.B. Leibiger, P.O. Berggren, Noninvasive high-resolution in vivo imaging of cell biology in the anterior chamber of the mouse eye, Nat. Protoc. 3 (2008) 1278–1286.
[50] A. Zimmer, J. Kreuter, J.R. Robinson, Studies on the transport pathway of PBCA nanoparticles in ocular tissues, J. Microencapsul. 8 (1991) 497–504.
[51] M.R. Prausnitz, J.S. Noonan, Permeability of cornea, sclera, and conjunctiva: a literature analysis for drug delivery to the eye, J. Pharm. Sci. 87 (1998) 1479–1488.
[52] K.G. Janoria, S. Gunda, S.H. Boddu, A.K. Mitra, Novel approaches to retinal drug delivery, Expert Opin. Drug Deliv. 4 (2007) 371–388.
[53] B.G. Short, Safety evaluation of ocular drug delivery formulations: techniques and practical considerations, Toxicol. Pathol. 36 (2008) 49–62.
[54] K. Hosoya, V.H. Lee, K.J. Kim, Roles of the conjunctiva in ocular drug delivery: a review of conjunctival transport mechanisms and their regulation, Eur. J. Pharm. Biopharm. 60 (2005) 227–240.
[55] S.B. Koevary, Pharmacokinetics of topical ocular drug delivery: potential uses for the treatment of diseases of the posterior segment and beyond, Curr. Drug Metab. 4 (2003) 213–222.
[56] A. Lambiase, P. Tirassa, A. Micera, L. Aloe, S. Bonini, Pharmacokinetics of conjunctivally applied nerve growth factor in the retina and optic nerve of adult rats, Invest. Ophthalmol. Vis. Sci. 46 (2005) 3800–3806.
[57] K. Mizuno, T. Koide, N. Saito, M. Fujii, M. Nagahara, A. Tomidokoro, Y. Tamaki, M. Araie, Topical nipradilol: effects on optic nerve head circulation in humans and periocular distribution in monkeys, Invest. Ophthalmol. Vis. Sci. 43 (2002) 3243–3250.

Drug Nanocrystals: Their Physicochemical Properties and Production Technologies

Koichi Baba* and Kohji Nishida

Department of Ophthalmology, Osaka University Graduate School of Medicine, Osaka, Japan

Received: 25 April 2011; Revised: 11 June 2011; Accepted: 06 July 2011

Abstract: In this review article are introduced some current topics concerning drug nanocrystals related to their physicochemical properties and production technologies with reference to patents. The physicochemical properties of nanonized drugs (i.e. drug nanocrystals) are individual, unique, and different from those of micronized drugs. As a result, drug nanocrystals have some superior pharmaceutical properties compared with their micronized equivalents (e.g. improved solubility and bioavailability). Already some drug nanocrystal products are commercially available. Drug nanocrystallization is an innovative formulation principle mainly for poorly soluble drugs. The special features of drug nanocrystals and their production technologies are described.

Keywords: Bottom-up technology, cancer therapy, combination technology, drug nanocrystals, homogenization technique, laser ablation technique, milling technique, nanomedicine, nanoparticles, nano spray dryer, ophthalmology, photodynamic therapy, precipitation technique, spray dryer technique, top-down technology.

1. INTRODUCTION

Recently, the application of nanotechnologies to nanomedicine has attracted considerable attention [1]. Especially, the expected contribution of nanoparticle technologies to nanomedicine has been greatly increasing. Numerous patents and research articles related to nanoparticles are already available such as tissue-imaging agents using metal nanoparticles [2-6], quantum dots for bioimaging [7-11], and nanoparticles used for tissue engineering [12-15] and drug delivery systems [16-25]. Among them, recently drug nanocrystals have been extensively researched since such formulations can improve pharmaceutical performance as well as resolve many intrinsic problems involving pharmaceutical agents [26]. One particularly serious matter with pharmaceuticals is that many drugs are hydrophobic with little water solubility. For example, approximately 40% of drugs in development phase and 70% of those undergoing production or screening are poorly soluble in aqueous media and even in organic solvents [27]. Poor drug solubility causes several drug delivery problems such as low oral bioavailability, erratic absorption, and impractical intravenous injection since large solvent volumes are required for hydrophobic drug administration, which may heighten the risk of side effects [28, 29].

To overcome these disadvantages, enthusiastic efforts have been taken to increase aqueous solubility of hydrophobic drugs by means of increasing the surface area of bulky drug powders; to this end micronized drug particles with sizes ranging at 1-10 μm have been fabricated. However, although micronized drug particles have increased dissolution velocity in aqueous media, this technique may not always overcome the bioavailability problems associated with very poorly soluble drugs [30]. In consequence, nanonization to even smaller size scales than micronization has been developed as an alternative approach, i.e. production of drug nanocrystals [31, 32].

It is notable that the speed of introduction of nanocrystals into the pharmaceutical market has been rapid. In the case of liposomes, in contrast, a period of about 25 years was necessary for their appearance in marketable pharmaceutical products [33]. Less than 10 years divided the filing of the first patent applications (1990s) [34] to the appearance on the market of the first nanocrystal drug product, Emend®, in 2000. This short time confirms that nanocrystal drugs are industrially feasible. Furthermore, accumulated knowledge and technological achievements in the drug nanoparticles during last decades may accrete the rapid transition of drug nanocrystals to the market. Nanocrystal serves as an ideal delivery system conferring high absorption for oral drugs and good suitability for intravenous injection as aqueous nanosuspensions [35]. Almost all the marketed products of nanocrystals currently are for oral administration as tablets and capsules (i.e. dry dosage forms) [28]. The therapeutic uses of these drugs are immunosuppressive, antiemetic, hypercholesterolemic, antianorexic, psychostimulant, and muscle relaxant. These drug nanocrystals demonstrate the importance of increased bioavailability through nanonization. More drugs having several administration routes such as oral, intrathecal, pulmonary, intravenous, and topical are currently under development [28]. The excellent reviews relating to commercially available products of drug nanocrystals are introduced by Müller *et al.* [28, 30].

This article will focus on some recent patents and the latest research related to drug nanocrystals including their unique physicochemical properties and production technologies; some future developments of drug nanocrystals are also described.

*Address correspondence to this author at the Department of Ophthalmology, Osaka University Graduate School of Medicine, 2-2 Yamadaoka, Suita, Osaka 565-0871, Japan; Tel: +81-6-6879-3456; Fax: +81-6-6879-3458; E-mail: koichi.baba@ophthal.med.osaka-u.ac.jp

1877-9131/11 $100.00+.00 © 2011 Bentham Science Publishers

2. PHYSICOCHEMICAL PROPERTIES OF DRUG NANOCRYSTALS INCLUDING THEIR NANOTOXICITY ASPECTS

Nanocrystals are basically made for drugs that are poorly soluble in water or water-soluble drugs as nanocrystals in oily medium. Especially for the purpose of intravenous targeting drug delivery, surface modification of drug nanocrystals are important, thus drug nanocrystals may be composed of other chemicals to act as drug carrier that have targeting ability [28]. Drug nanocrystals have particle sizes in the nanometer range and are a class of nanoparticles with crystalline characteristics. By definition, pharmaceutical nanoparticles have sizes ranging from a few nanometers to 1μm, whereas larger particles with sizes 1-1000μm are microparticles [30]. In general, stabilizers such as surfactants are necessary to disperse nanocrystals in aqueous media; the dispersion of drug nanocrystals in liquid media forms so-called nanosuspensions. Nanocrystals possess 100% drug loading, in contrast to carrier-based nanoparticles such as polymers [36], nanoemulsions [37, 38], liposomes [39, 40], and lipid nanoparticles [41] (i.e. high drug loading in nanocrystal formulation). Regarding physicochemical properties, nanocrystals have special features of increased saturation velocity, dissolution velocity, and drug adhesiveness to cell membranes, leading to sufficiently high therapeutic drug concentrations for the requisite pharmacological effect [42]. The physical background of these effects (e.g. equations by Kelvin, Ostwald-Freundlich) has been described in detail elsewhere in the literature [43-45]. Thus nanocrystals have potential to solve many biopharmaceutical delivery problems of poorly soluble drugs such as low bioavailability after oral administration, low dermal penetration, and large injection volume required for intravenous administration as well as undesirable side effects following intravenous injection using solubilizing agents. Drug nanocrystal formulation can achieve reproducible oral and dermal absorption, improve bioavailability and dose-proportionality, and increase patient compliance due to lowering numbers of oral units to be taken [46].

On the other hand, nanoparticles also imply nanotoxicity. Research (largely using small animals) to date on the potential ill effects of nanoparticles have concentrated on exposure by inhalation, with damage conferred not only on the lung but possibly by transfer *via* the blood stream to other organs. There is some evidence that single-walled carbon nanotubes may behave like asbestos fibers and confer risk of inflammation and formation of lesions known as granulomas [47, 48]. Overall, considering the effects of particle size, degradability versus biopersistency and intracellular uptake, drug nanocrystals are basically classified low- or non-risk agents, especially in the case of those administered topically or orally [49]. However, in contrast, intracellular uptake plays a key role after intravenous injection of drug nanocrystals [49]. Uptake of drug nanocrystals by phagocytic mononuclear cells (e.g. in the liver) can cause cytotoxicity in case of too high nanocrystal concentrations in the macrophages. The balance between uptake of drug nanocrystals by mononuclear phagocytic system cells and target cells is critical for successful therapy. Very little research has been done on nanotoxicology of drug nanocrystals, and so far empirical approaches have been predominantly undertaken. Further systemic investigations of nanotoxicity of drug nanocrystals are necessary.

3. PRODUCTION TECHNOLOGIES OF DRUG NANOCRYSTALS

To date, two basic approaches for producing drug nanocrystals have been mainly developed: top-down technologies (reducing large-sized drug powders to smaller sizes by e.g. mechanical stress) and bottom-up technologies (e.g. controlled precipitation to form crystals or amorphous particles). The types of production techniques are summarized in Table 1.

Table 1. Production Technologies of Drug Nanocrystals

		Ref. No.
Top-down	Milling	[50-55]
	Homogenization	[56-60]
	Laser ablation	[61-67]
Bottom-up	Precipitation	[68-84]
	Spray dryer	[85-91]
Combination	Precipitation & Homogenization	[92-97]

3.1. Top-Down Technologies

3.1.1. Milling Techniques

Using top-down technologies large crystals in the micrometer-to-millimeter size range are reduced to nanosize by grinding (e.g. using a milling process) [50, 53]. Since dry milling is not efficient to obtain particle sizes in the nanometer range, wet milling is predominantly applied. In wet milling process drug particles are dispersed in a surfactant and/or stabilizer solution as macrosuspensions then subjected to milling energy to produce a nanosuspension. A low-energy milling process technology using the pearl mill (bead mill) was developed as NanoCrystal™ technology [54, 55]. Using this technology a suspension is added to a milling container containing milling pearls, typically sized 0.2 or 0.4-0.6mm. The pearls, moved by an agitator, grind the crystals to produce a nanosuspension. Several types of drug nanocrystals produced using pearl mill technology are currently on the market, mostly provided as formulations for oral administration.

3.1.2. Homogenization Techniques

Crystals can be ground by a high-energy process using high-pressure homogenization [56]. In this process crystals in suspension are rendered into smaller sizes by means of high-energy fluid streams causing the collision and cavitation [57, 58]. Ezetimibe nanocrystals are an example of a product obtained by this homogenization technique [59]. The preparation method uses ultrasonic or mechanical high-speed homogenization. An alternative high-energy method uses piston-gap homogenizers [60]. In this process the suspension is passed at high velocity through a small gap.

Inside the gap, the crystals are milled by force of cavitation, collision, and shear forces of the liquid. These homogenization processes are normally carried out with water suspensions, although homogenization in water-free media such as oils and liquid polyethylene glycols or water-reduced media is also possible. Oil dispersions can directly be filled into gelatin capsules for oral administration, or injected parenterally as controlled drug delivery depot.

3.1.3. Laser Ablation Techniques

Recently, novel femtosecond (fs) laser techniques for fabricating drug nanocrystals in aqueous medium have been developed. The process is implemented after adding a poorly water-soluble or water-insoluble medicinal ingredient of a drug into a poor solvent (e.g. water) to form a suspension, followed by laser irradiation (Fig. 1). The controlled power of ablation and the fragmentation caused by laser irradiation are key points for fabricating fine size-controlled nanocrystals. For example, optimal laser fragmentation conditions generated uniformly size-controlled paclitaxel nanoparticles (<500nm) with quantifiable degradation [61]. The particle size and the drug concentration are optimally tuned. Generally, laser treatment at higher powers produces smaller particles with larger amounts of degradation. Using the laser ablation technique drug nanocrystals can be produced in quite small quantities, which may be a useful advantage for preclinical evaluation of new drug candidates. The drug nanoparticles have high purity and may exhibit high bioavailability when used as medicines, agricultural chemicals, or chemical fertilizers [62].

Ryo *et al.* [63] disclosed the production of dispersion solution of organic nanoparticles using laser ablation, where the suspension was prepared by dispersing hydrophobic organic compounds in a poor solvent (e.g. water). By this method, a preparation of the anti-ulcerative colitis drug salazosulfapyridine nanocrystals has been demonstrated [63]. The type of medicinal ingredient may also include anticancer drugs (ellipticine, camptothecin), vitamins, analgesics, and anti-inflammatory drugs. Suitable laser irradiation devices include solid state laser such as YAG laser, titanium-sapphire laser, and ruby laser; gas laser such as excimer laser, argon (Ar) ion laser, and CO_2 laser; liquid laser such as a dye laser; and semiconductor laser such as a gallium arsenide (GaAs) laser. The appropriate amount of medicinal ingredient obtained in one batch may be 10-1000μg per 1ml of water. Scanning electron microscopy confirmed that ellipticine nanoparticles with a mean particle size approximately 100nm were obtained [64]. The anticancer drug camptothecin was also formulated by a similar process [65]. The flow device related to laser ablation equipment has been disclosed for the purpose of mass production [66]. In an informative review, Barcikowski *et al.* [67] evaluated the impact and structure of the field of laser ablation techniques and mapped global spots of their activities during 1998–2008 [67].

3.2. Bottom-Up Technologies

3.2.1. Precipitation Techniques

In bottom-up technologies, a precipitation process is the major approach used [68-73]. The basic principle is that first the drug is dissolved in a solvent then the solution is added to an insoluble medium (e.g. water) resulting in drug precipitation. The important points in this process are to control the structure of the particles (amorphous or crystalline) and to avoid crystal growth reaching the micrometer size range. The industrially relevant technologies of various precipitation processes are patented by BASF Corporation. For example, the patents describe the production of carotenoid preparations in the form of cold-water dispersible powders [74, 75] and precipitated water-insoluble colorants in colloid-dispersed form [76] and are exploited in products for food and soft drink industry. The precipitation process can be carried out so that amorphous nanoparticles result. Another process leading to crystalline nanoparticles was developed by Novartis to produce so-called hydrosols [77]. A novel advanced precipitation technique for preparing nanoparticles as medicines, cosmetics, and foods uses supercritical fluid [78]. Alternately, there are various other bottom-up technologies such as the sonocrystallization, high-gravity controlled-precipitation technology, multi-inlet vortex mixing, and confined impinging liquid jet precipitation; a detailed review of these techniques is provided by Müller *et al.* [49].

Recently, Prasad's group [79, 80] demonstrated a novel type of photodynamic cancer therapy using a pure nanocrystal form of drugs produced by the precipitation technique [79,80]. Water-insoluble sensitizing drugs were successfully nanocrystallized by the precipitation procedure. The obtained drug nanocrystals had fine and stable water dispersion even with surfactant– and organic solvent-free conditions. Although this was a candidate carrier-free novel

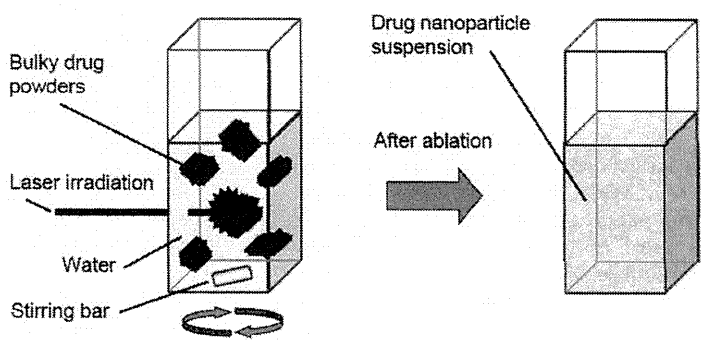

Fig. (1). Scheme of laser ablation technique.

drug delivery method using pure nanocrystalline form of hydrophobic drugs for photodynamic cancer therapy, the nanocrystals thus obtained showed fluorescence quenching caused by drug crystallization in aqueous dispersion medium. Therefore, this nonphotoactive property of drug nanocrystals seemed unsuitable for photodynamic cancer therapy. However, there was an interesting finding in that these water-insoluble drug nanocrystals showed good solubility in a serum contained aqueous medium. As a result, a dye molecule, which was generated from drug nanocrystals dissolved *in vitro* and *in vivo,* successfully recovered its photosensitizing activity. Laser-irradiated dyes owe their activity to the generation of singlet oxygen species that cause irreversible damage to tumors. This drug nanocrystal dissolution was not observable in pure water; thus lipoprotein or some hydrophobic components in serum may allow the dissolution mechanism possibly by hydrophobic-hydrophobic interactions between serum components and nanocrystals. This unique feature of organic nanocrystals was also adapted to cultured living cell bioimaging *in vitro* using fluorescent organic nanocrystals [81, 82]. Additionally, as our current research interest, nanoparticle eye drops having high ocular penetration that enable fluorescence imaging of the ocular globe by confocal laser fluorescence microscopy were successfully prepared by precipitation techniques [83, 84].

3.2.2. Spray-Drying Techniques

Spray-drying techniques can be classified as a bottom-up technology [85]. In this process drugs dissolved in water/organic solvents are electrosprayed as a very fine mist and thereby form nanoparticles by evaporation of the water/organic solvent. The average size of particles obtained by conventional spray dryer is from a few micrometers to hundreds of micrometers. There are several variations, e.g. protein-coated bioactive nanoparticle suspension using electro-spraying apparatus [86]. Generally, however, production of nanoparticles <1μm in size is difficult using a conventional spray dryer.

Recently, Büchi Corporation (Flawil, Switzerland) invented a novel spray dryer, the Nano Spray Dryer B-90 (Fig. 2), launched in 2010 [87]. The key point of this equipment is the use of piezoelectric effect in vibrating mesh spray technology for fabricating small-sized droplets. The size of nanocrystals thus obtained is usually in the rage 300-1000 nm. Using the Nano Spray Dryer B-90 a model microparticle vehicle suitable for respiratory delivery of biological pharmaceutical actives was designed. To enhance its aerosol dispersibility, L-leucine was chosen as one of the excipients; trehalose was the second excipient [88]. The preparation of protein nanoparticles was demonstrated [89]. β-Galactosidase was chosen as model protein and trehalose added as stabilizer. The selected condition of running process significantly influenced activity of the obtained enzyme and also increased its stability in storage. Alternatively, a simpler approach for the production of protein nanoparticles for a variety of drug delivery applications was introduced [90]. Five representative polymeric wall materials (gum arabic, whey protein, polyvinyl alcohol, modified starch, and maltodextrin) for the encapsulated nano-emulsions as well as formulating nanocrystals (e.g. from furosemide) were investigated [91].

Recently, our interest has focused on preparation of drug nanoparticle eye drops using nanospray dryer equipment. A steroid compound, dexamethasone, was selected as model compound, and fine nanoparticles were successfully prepared (Fig. 3). Based on this encouraging result, several kinds of ophthalmic drugs are now under investigation as candidates for drug nanoparticle eye drops. Such eye drops prepared by nanospray dryer are expected to increase the drug's ocular penetration and efficacy. As such, nanoparticle eye drops maybe useful against several kinds of eye diseases including refractory lesions such as Fuchs corneal endothelial dystrophy.

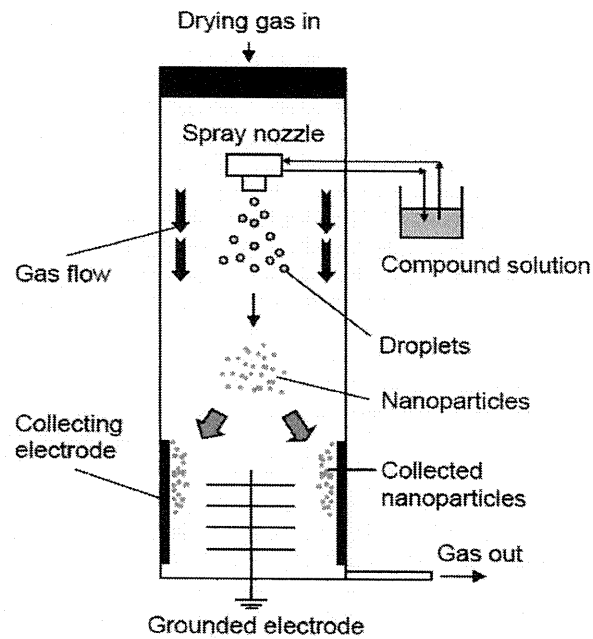

Fig. (2). Scheme of nanospray dryer system.

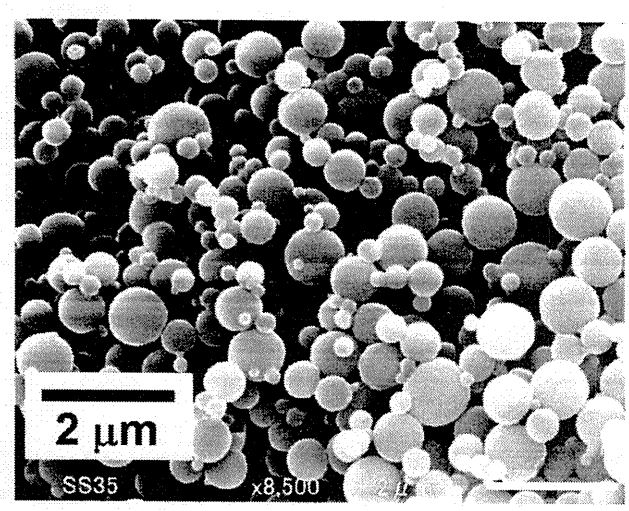

Fig. (3). Dexamethasone nanoparticles prepared by Nano Spray Dryer B-90 (Büchi Corporation, Flawil, Switzerland). Dexamethasone dissolved in ethanol (50 mg/30 ml) was spray-dried at 50°C for 2 h running time. The spray nozzle size was 4.0μm.

3.3. Combination Technologies

Drug nanocrystal-producing combination technologies employ a blend of bottom-up and top-down methodologies. For example, crystals precipitated in suspension may be subjected to a high-energy process, typically high-pressure homogenization [92,93], followed by counter-flow precipitation process whereby the solvent and non-solvent are mixed in two counter flows resulting in crystal precipitation [94]. One of the advantages of this combination technique is that can produce very small nanocrystals <100 nm in size. Such small nanocrystals are difficult to obtain by means of conventional top-down technologies using pearl milling or simple high-pressure homogenization, especially in large-scale industrial production.

Preparations for topical application containing nanocrystals of cosmetically active ingredients have been disclosed [95]. The purpose of this invention is to attain increased bioactivity of molecules in the skin and thereby enhance cosmetic preparations. The nanocrystals can be added to any cosmetic topical formulation such as lotions, creams, and liposomal dispersions. These cosmetic drug nanocrystals are produced by a combination process of low-energy pearl milling followed by high-energy, high-pressure homogenization leading to nanocrystal suspensions with excellent physical stability. Another combination process employs cavitation, instead of precipitation, followed by high-pressure homogenization [96]. Combination techniques of supercritical fluid and spraying are disclosed for the production of fine particles without using carrier particles and binder as foreign substance [97].

4. CURRENT AND FUTURE DEVELOPMENTS

We introduced current topics of patents and recent research related to drug nanocrystals with their physicochemical properties and production technologies. Since drug nanocrystals have some superior characteristics based on their peculiar physiochemical properties compared with conventional micronized drugs, several pharmaceutical benefits are expected (e.g. less solubility problems, improved bioavailability, increased patient compliance due to lower/less frequent dosing). Already, several kinds of drug nanocrystals are commercially available, and a number of new drug nanocrystals are under development. The nanocrystal formulation of drugs is a kind of universal approach for drug molecules. Additionally, surface modification of drug nanocrystals will extend the drug bioavailability by means of achieving prolonged release and targeted drug delivery. The production technologies will be increasingly more sophisticated along with the development of current technology (i.e. achievement of mass production with low cost, which will be accelerated by new patents), and the market for drug nanocrystals will be thus extended to include not only drugs but also cosmetics and nutritional products. There is much room for further research in these areas. For instance, nanotoxicological studies of drug nanocrystals should be extensively carried out. Such investigations are essential for the better understanding of drug nanocrystals on the cellular level and can also open new avenues for nanocrystal applications. Increased knowledge the intracellular fate of nanocrystals could lead to many new treatment approaches.

ACKNOWLEDGEMENTS

This study was partially supported by Health and Labor Science Research Grants for Research on Intractable Diseases from the Ministry of Health, Labor and Welfare of Japan.

CONFLICT OF INTEREST

Author does not have any conflict of interest to declare.

REFERENCES

[1] Freitas RA Jr. Current Status of Nanomedicine and medical nanorobotics. J Comput Theor Nanosci 2005; 2; 1-25.
[2] Porter MD. Raman-active reagents and the use thereof. US7829348, 2010.
[3] Lee JH, Seo WS, Dai H, Liu Z, Sherlock SP. Multifunctional metal-graphite nanocrystals. US20080213189, 2008.
[4] Gao M, Hu F, Liu S, Lu X. Biocompatible magnetic nanocrystals and powder bearing a surface reactive group. US20080203351, 2008.
[5] Shin DY, Kim JS. Anti-cancer medicine both for diagnosing and treating cancer. WO2008146976, 2008.
[6] Chung DS, Kang K, Jeon Y, Kim Y, Alothman ZA, Ahmed AYH, Choi K, Aimajid AM, Piao J, Alothman AA, Quan B. Fluorescent sillica Nanoparticle with raduiactuve tag and the detecting method of pte and fluorescent dual imaging using thereof. WO2010030120, 2010.
[7] Tulsky E, Bartel J, Treadway J. Methods for preparation of ZnTe nanocrystals. WO2010040032, 2010.
[8] Bartel J, Chen Y, Tulsky E, Treadway J. Stable indium-containing semiconductor nanocrystals non-toxic to cells and tissues. WO2010003059, 2010.
[9] Brogan L, Liu W. Semiconductor nanocrystal complexes and methods of detecting molecular interactions using same. WO2006084013, 2006.
[10] Empedocles SA, Watson AR. Single target counting assays using semiconductor nanocrystals. WO2001061348, 2001.
[11] Barbera-Guillem E. Functionalized nanocrystals as visual tissue-specific imaging agents, and methods for fluorescence imaging. WO2000027436, 2000.
[12] Ikoma T, Yoshioka T, Tonegawa T, Tanaka J, Abe T, Sakane M, Ochial N. Controlled-release drug preparation and method for producing the same. WO2008007796, 2008.
[13] Bumgardner JD, Chesnutt BM, Haggard WO, Yuan Y, Utturkar TM, Reves B. Chitosan/nanocrystalline hydroxyapatite composite microsphere-based scaffolds for bone engineering. US20070254007, 2007.
[14] Fowler C, Parkinson CR. Oral compositions comprising rod-shaped apatite nanocrystals for combating dental erosion. WO2007065856, 2007.
[15] Luo TJM, Ko CC, Tulloch C. Formable bioceramics comprising hydroxyapatite nanocrystals and gelatin for bone repairs and tissue engineering. US20100178278, 2010.
[16] De Los Rios MA, Oh KJ, Bullock TL, Johnson PT, Ostrowski J. Self-assembling nanoparticle drug delivery system containing hepatitis B virus core protein conjugates with polylysine and/or polyhistidine and lipids. WO2008124165, 2008.
[17] Stevens, Molly M.; Ulijn, Rein; Laromaine, Sague Anna; Koh, Liling. Enzyme-cleavable nanoparticle aggregate for diagnostic and drug delivery use. WO2007063300, 2007.
[18] Manneh V. Therapeutic nanoconjugates. WO2009038776, 2009.
[19] Nelson T, Quattrone A, Alkon D. Artificial low-density lipoprotein carriers for transport of substances across the blood-brain barrier. US7514402, 2009.
[20] Baranova AV. Nanogenomics for medicine, siRNA engineering. US20090306185, 2009.
[21] Leary JF, Prow TW. Multilayered nanomedical drug/gene delivery system. WO05084326, 2005.
[22] Clarke JT, Weber J, Flanagan A. Drug-delivery balloons. US20110160659, 2011.
[23] Sung HW, Liang HF, Tu H. Nanoparticles for protein drug delivery. US7871990, 2011.

[24] Cunningham J, Liversidge EM. Nanoparticulate compositions having a peptide as a surface stabilizer. US7879360, 2011.
[25] Ceve G, Chopra A, Stieber J. Methods of transnasal transport/immunization with highly adaptable carriers. US7927622, 2011.
[26] Nagarwal RC, Kumar R, Dhanawat M, Das N, Pandit JK. Nanocrystal technology in the delivery of poorly soluble drugs: An overview. Current Drug Delivery 2011; 8; 398-406.
[27] Merisko-Liversidge EM, Liversidge GG. Drug nanoparticles: formulating poorly water-soluble compounds. Toxicol Pathol 2008; 36; 43-8.
[28] Shegokar R, Müller RH. Nanocrystals: Industrially feasible multifunctional formulation technology for poorly soluble actives. Int J Pharm 2010; 399; 129-39.
[29] Willems L, van der Geest R, de Beule K. Itraconazole oral solution and intravenous formulations: a review of pharmacokinetics and pharmacodynamics. J Clin Pharm Ther 2001; 26; 159-69.
[30] Junghanns JUAH, Müller RH. Nanocrystal technology, drug delivery and clinical applications. Int J Nanomedicine 2008; 3(3); 295-309.
[31] Gao L, Zhang D, Chen M. Drug nanocrystals for the formulation of poorly soluble drugs and its application as a potential drug delivery system. J Nanopart Res 2008; 10; 845-62.
[32] Rabinow BE. Nanosuspensions in drug delivery. Nat Rev Drug Discov 2004; 3; 785-96.
[33] Diederichs JE, Müller RH. Liposome in kosmetika und arzneimitteln. Pharm Ind 1994; 56; 267-75.
[34] Müller RH, Becker R, Kruss B, Peters K. Pharmaceutical nanosuspensions for medicament administration as systems with increased saturation solubility and rate of solution. US5858410, 1999.
[35] Rabinow B, Kipp J, Papadopoulos P, Wong J, Glosson J, Gass J, Sun CS, Wielgos T, White R, Cook C, Barker K, Wood K. Itraconazole IV nanosuspension enhances efficacy through altered pharmacokinetics in the rat. Int J Pharm 2007; 339; 251-60.
[36] Couvreur P, Tulkens P, Roland M, Trouet A, Speiser P. Nanocapsules: a new type of lysosomotropic carrier. FEBS Lett 1977; 84; 323-26.
[37] Müller RH, Heinemann S. Emulsions for intravenous administration. I. Emulsions for nutrition and drug delivery. Pharm Ind 1993; 853-56.
[38] Collins-Golda LC, Lyonsa RT, Bartholow LC. Parenteral emulsions for drug delivery. Adv Drug Deliv Rev 1990; 5; 189-208.
[39] Storm G, Wilms HP, Crommelin DJ. Liposomes and biotherapeutics. Biotherapy 1991; 3; 25-42.
[40] Crommelin DJ, Storm G. Liposomes: from the bench to the bed. J Liposome Res 2003; 13; 33-6.
[41] Müller RH, Shegokar S, Keck CM. 20 Years of Lipid Nanoparticles (SLN and NLC): Present State of Development and Industrial Applications. Curr Drug Discov Technol 2011.
[42] Müller RH, Gohla S, Keck CM. State of the art of nanocrystals - Special features, production, nanotoxicology aspects and intracellular delivery. Eur J Pharm Biopharm 2011; 78; 1-9.
[43] Buckton G, Beezer AE. The relationship between particle size and solubility. Int J Pharm 1992; 82; R7-10.
[44] Möschwitzer J, Müller RH. New method for the effective production of ultrafine drug nanocrystals. J Nanosci Nanotech 2006; 6; 3145-53.
[45] Keck CM, Müller RH. Smart crystals - review of the second generation of drug nanocrystal. In: Torchilin VP, Amiji MM, Eds. Handbook of materials for nanomedicine. Pan stanford series on biomedical nanotechnology. Pan Stanford Publishing 2010: pp. 555-80.
[46] Rabinow B. Pharmacokinetics of drugs administrated in nanosuspension. Discov Med 2005; 5; 74-9.
[47] Dawson TL. Nanomaterials for textile processing and photonic applications. Color Technol 2008; 124; 261-72.
[48] Poland CA, Duffin R, Kinloch I, *et al.* Carbon nanotubes introduced into the abdominal cavity of mice show asbestos-like pathogenicity in a pilot study. Nat Nanotechnol 2008; 3; 423.
[49] Müller RH, Gohla S, Keck CM. State of the art of nanocrystals - Special features, production, nanotoxicology aspects and intracellular delivery. Eur J Pharm Biopharm 2011; 78; 1-9.
[50] Dodd A, Meiser F, Russell A, Norret M, Bosch HW. Production of encapsulated nanoparticles at commercial scale. WO2010121322, 2010.
[51] Bruno JA, Doty BD, Gustow E, Illig KJ, Rajagopalan N, Sarpotdar P. Method of grinding pharmaceutical substances. US5518187, 1996.
[52] Liversidge G, Jenkins S, Liversidge EM. Injectable nanoparticulate olanzapine formulations. US7910577, 2011.
[53] Ryde T, Gustow EE, Ruddy SB, Jain R, Patel R, Wilkins MJ. Nanoparticulate fibrate formulations. US7931917, 2011.
[54] Liversidge GG, Cundy KC. Particle size reduction for improvement of oral bioavailability of hydrophobic drugs: I. Absolute oral bioavailability of nanocrystalline danazol in beagle dogs. Int J Pharm 1995; 125; 91-7.
[55] Merisko-Liversidge E, Liversidge GG, Cooper ER. Nanosizing: a formulation approach for poorly-water-soluble compounds. Eur J Pharm Sci 2003; 18; 113-20.
[56] Müller RH, Krause K, Mader K. Method for controlled production of ultrafine microparticles and nanoparticles. WO2001003670, 2001.
[57] Khan S, Pace GW. Composition and method of preparing microparticles of water-insoluble substances. US6337092, 2002.
[58] Majuru S, Oyewumi MO. Nanotechnology in drug development & life cycle management. In: de Villiers MM, Aramvit P, Kwon GS, Eds. Nanotechnology in Drug Delivery: 10 (Biotechnology: PharmaceuticalAspects). Springer: American Association of Pharmaceutical Scientists 2009: pp. 597-620.
[59] Oner L, Gursoy RN, Gulsun T. Method for the preparation of ezetimib nanocrystals. WO2010144066, 2010.
[60] Müller RH, Krause K, Mäder, K. Method for controlled production of ultrafine microparticles and nanoparticles. WO2001003670, 2001.
[61] Kenth S, Sylvester JP, Fuhrmann K, Meunier M, Leroux JC. Fabrication of paclitaxel nanocrystals by femtosecond laser ablation and fragmentation. J Pharm Sci 2011; 100; 1022-30.
[62] Nagare S. Drug nanoparticles, method and apparatus for preparing pharmaceutical preparation using the particles. WO2004110405, 2004.
[63] Ryo S, Oh I, Sugiyama T, Izumi E. Manufacturing method and apparatus for organic compound nanoparticle dispersion solution. JP2010234218, 2010.
[64] Asahi T, Masuhara H, Sugiyama T, Oh I, Ryo S, Kato H, Umeda I. Method of producing medicinal nanoparticle suspension. US7597278, 2009.
[65] Asahi T, Sugiyama T, Masuhara H. Laser fabrication and spectroscopy of organic nanoparticles. Acc Chem Res 2008; 41; 1790-8.
[66] Kato H, Umeda I, Asahi T, Masuhara H, Sugiyama T, Oh I, Ryo S, Hirata K, Nohmi M. Apparatus for forming ultrafine particles. US7815426, 2010.
[67] Barcikowski S, Devesa F, Moldenhauer K. Impact and structure of literature on nanoparticle generation by laser ablation in liquids. J Nanopart Res 2009; 11; 1883-93.
[68] Tabibi SE, Ezennia EI, Vishnuvajjala BR, Gupta S. Water-insoluble drug delivery system. WO2000037050, 2000.
[69] Kipp JE, Wong JCT, Doty MJ, Rebbeck CL, Brynjelsen S, Werling J, Sriram R. Method for preparing submicron particle suspensions. WO2002055059, 2002.
[70] Kipp JE, Wong JCT, Doty MJ, Rebbeck CL. Microprecipitation method for preparing submicron suspensions. US6869617, 2005.
[71] Moeschwitzer J. Method for producing ultrafine submicronic suspensions. WO2006094808, 2006.
[72] Möschwitzer JP. Embedded micellar nanoparticles. US7923026, 2011.
[73] Niesz K, Wootsch A, Groualle M, Ötvös Z, Darvas F. Instrument and process for nanoparticles production in continuous flow mode. US20110104043, 2011.
[74] Runge F, Auweter H, Musaeus-Jensen N, Haberkorn H, Rieger J. Stable, pulverulent lycopene formulations, comprising lycopene having a degree of crystallinity of greater than 20%, US6235315, 2001.
[75] Auweter H, Bohn H, Luddecke E. Stable, aqueous dispersions and stable, water-dispersible dry xanthophyll powder, their production and use, US6296877, 2001.

[76] Auweter H, Bohn H, Heger R, Horn D, Siegel B, Siemensmeyer K. Precipitated water-insoluble colorants in colloid disperse form. US6494924, 2002.

[77] List M, Sucker H. Pharmaceutical colloidal hydrosols for injection, GB2200048, 1988.

[78] Kim KS, Cho YT. Preparation of nanoscale particles using supercritical fluids. WO2007129829, 2007.

[79] Prasad PN, Pudavar HE, Bbaba K, Roy I, Ohulchanskyy T, Pandey RK, Oseroff A. Method for Delivering Hydrophobic Drugs *via* Nanocrystal Formulations. WO2008048205, 2008.

[80] Baba K, Pudavar HE, Roy I, *et al.* A New method for delivering a hydrophobic drug for photodynamic therapy using pure nanocrystal form of the drug. Mol Pharmaceutics 2007; 4(2); 289-97.

[81] Prasad PN, Baba K, Pudavar H, Roy I, Ohulchanskyy T, Nakanishi H, Masuhara A, Kasai H. Method of bioimaging using nanocrystals of fluorescent dyes. WO2008054341, 2008.

[82] Baba K, Kasai H, Masuhara A, Oikawa H, Nakanishi H. Organic solvent-free fluorescence confocal imaging of living cells using pure nanocrystal forms of fluorescent dyes. Jpn J Appl Phys 2009; 48; 117002.

[83] Nishida K, Baba K, Kasai H, Tanaka Y, Kubota A, Yokokura S. Eye drop having high intraocular migration properties, fluorescent imaging agent, and methods for producing same. WO2010053101, 2010.

[84] Baba K, Tanaka K, Kubota A, Kasai H, Yokokura S, Nakanishi H, Nishida K. A method for enhancing the ocular penetration of eye drops using nanoparticles of hydrolysable dye. J Control Release 2011; in press.

[85] Pui DYH, Chen DR. High mass throughput particle generation using multiple nozzle spraying. US7498063, 2009.

[86] Pui DYH, Chen DR. Electrospraying apparatus and method for coating particles. US7279322, 2007.

[87] Schmidl K, Arpagaus C, Friess W. Evaluation of the nano spray dryer B-90 for pharmaceutical applications. Pharm Dev Technoly 2011; 16(4); 287-94.

[88] Feng AL, Boraey MA, Gwin MA, Finlay PR, Kuehl PJ, Vehring R. Mechanistic models facilitate efficient development of leucine containing microparticles for pulmonary drug delivery. Int J Pharm 2011; 409; 156-63.

[89] Bürki K, Jeon I, Arpagaus C, Bets G. New insights into respirable protein powder preparation using a nano spray dryer. Int J Pharm 2011; 408; 248-56.

[90] Lee SH, Heng D, Ng WK, Chan HK, Tan RBH. Nano spray drying: a novel method for preparing protein nanoparticles for protein therapy. Int J Pharm 2011; 403; 192-200.

[91] Li X, Anton N, Arpagaus C, Belleteix F, Vandamme TF. Nanoparticles by spray drying using innovative new technology: The Büchi Nano Spray Dryer B-90. J Control Release 2010; 147; 304-10.

[92] Kipp JE, Wong JCT, Doty MJ, Rebbeck CL, Microprecipitation method for preparing submicron suspensions. US6607784, 2003.

[93] Berney RL. Formulations of px compounds. US20110097410, 2011.

[94] Kipp JE, Wong JCT, Doty MJ, Werling J, Rebbeck CL, Brynjelsen S. Method for preparing submicron particle suspensions. US6884436, 2005.

[95] Petersen R. Nanocrystals for use in topical cosmetic formulations and method of production thereof. US20100047297, 2010.

[96] Müller RH, Möschwitzer J. Method and device for producing very fine particles and coating such particles. US20090297565, 2009.

[97] Watano S. Method of granulating fine particles. WO2006046670, 2006.